The impact of training on the inner–outer asymmetry in crowding

Yan-Ru Chen

School of Psychological and Cognitive Sciences and Beijing Key Laboratory of Behavior and Mental Health, Peking University, Beijing, China

✉

Yu-Wei Zhang

School of Psychological and Cognitive Sciences and Beijing Key Laboratory of Behavior and Mental Health, Peking University, Beijing, China

✉

Jun-Yun Zhang

School of Psychological and Cognitive Sciences and Beijing Key Laboratory of Behavior and Mental Health, Peking University, Beijing, China

✉

Inner–outer asymmetry, where the outer flanker induces stronger crowding than the inner flanker, is a hallmark property of visual crowding. It is unclear the contribution of inner–outer asymmetry to the pattern of crowding errors (biased predominantly toward the flanker identities) and the role of training on crowding errors. In a typical radial crowding display, 20 observers were asked to report the orientation of a target Gabor (7.5° eccentricity) flanked by either an inner or outer Gabor along the horizontal meridian. The results showed that outer flanker conditions induced stronger crowding, accompanied by assimilative errors to the outer flanker for similar target/flanker elements. In contrast, the inner flanker condition exhibited weaker crowding, with no significant patterns of crowding errors. A population coding model showed that the flanker weights in the outer flanker condition were significantly higher than those in the inner flanker condition. Nine observers continued to train the outer flanker condition for four sessions. Training reduced inner–outer asymmetry and reduced flanker weights to the outer flanker. The learning effects were retained over 4 to 6 months. Individual differences in the appearance of crowding errors, the strength of inner–outer asymmetry, and the training effects were evident. Nevertheless, our findings indicate that different crowding mechanisms may be responsible for the asymmetric crowding effects induced by inner and outer flankers, with the outer flankers dominating the appearance more than the inner ones. Training reduces inner–outer asymmetry by reducing target/flanker confusion, and learning is persistent over months, suggesting that perceptual learning has the potential to improve visual performance by promoting neural plasticity.

Introduction

Crowding is the inability of recognizing an object with the presence of adjacent objects (or flankers) in the normal periphery and central vision in disorders such as amblyopia (Levi & Klein, 1985). It is considered to be an essential bottleneck or breakdown of object recognition (Strasburger, Rentschler, & Juttner, 2011; Whitney & Levi, 2011). Recent studies have established several diagnostic characteristics to distinguish crowding from other effects, such as masking, lateral interaction, and surround suppression (Levi, 2008; Whitney & Levi, 2011). One of the hallmark characteristics is inner–outer asymmetry, which demonstrates that the outer flanker (farther away from the fovea relative to the target) produces stronger interference than the inner one (closer to the fovea) (Bouma, 1970; Bouma, 1973). This seems unreasonable, as the inner flanker should be more distinguishable because of the better acuity for objects closer to the fovea and thus should be a stronger flanker. The inner–outer asymmetry has been found in different types of stimuli and tasks, such as Gabor orientation discrimination, letter recognition, and face recognition (Banks, Bachrach, & Larson, 1977; Bex, Dakin, & Simmers, 2003; Bouma, 1973; Farzin, Rivera, & Whitney, 2009; Petrov, Popple, & McKee, 2007).

Crowding is often attributed to abnormal integration of signals over space (Levi, Klein, & Hariharan, 2002; Pelli, Palomares, & Majaj, 2004) or limited attention resolution (He, Cavanagh, & Intriligator, 1996; Intriligator & Cavanagh, 2001) because of insufficient spatial resolution to discern the target and flankers in the periphery. In terms of inner–outer

asymmetry, several theories have been provided to account for it. The early account is associated with the cortical magnification factor (Pelli, 2008). It has been observed that, although the angular separations for inner and outer flankers are the same in visual space, the outer flanker is closer to the target than the inner one after mapping to cortical space; therefore, the outer flanker has more interference with the target (Motter & Simoni, 2007). Others have argued that the inner–outer asymmetry can be ascribed to the fact that increased receptive field sizes in the periphery bias the sampling rate toward the outer flanker (Dayan & Solomon, 2010) or leads to sparse selection in the visual periphery (Chaney, Fischer, & Whitney, 2014). Alternatively, inner–outer asymmetry can be explained in terms of attention allocation, which suggests that the asymmetrical deployment of attention outward leads to the selection of an outer flanker (Petrov & Meleshkevich, 2011a; Petrov & Meleshkevich, 2011b).

The measurements of errors observers made when reporting the identity of crowded targets provide an effective way to understand the mechanisms of crowding. Various models have been proposed to explain the systematic shift in the identity of crowded targets and the different types of errors: either reporting flanker identity (substitution errors) or reporting intermediate identities between the target and flankers (assimilation errors). Substitution models postulate that observers often misreport a flanker, causing substitution errors (Ester, Klee, & Awh, 2014; Ester, Zilber, & Serences, 2015). This substitution is attributed to the increased location uncertainty in the periphery (Krumhansl, 1977; Wolford, 1975; Zhang, Zhang, Liu, & Yu, 2012) or unfocused spatial attention (Strasburger, 2005; Strasburger, Harvey, & Rentschler, 1991), rendering the observers' failure to spatially differentiate between the target and the flankers. On the other hand, pooling or averaging models postulate that observers simultaneously detect and pool excessive information of low-level features, including those that belong to the flankers under crowding, as a result of inappropriate integration field size in the periphery (Freeman & Simoncelli, 2011; Greenwood, Bex, & Dakin, 2009; Harrison & Bex, 2015; Harrison, Mattingley, & Remington 2012; Keshvari & Rosenholtz, 2016; Parkes, Lund, Angelucci, Solomon, & Morgan, 2001). Population pooling models, which sum up responses for target and flanker features with different weights, were proposed to explain the perceptual effects of crowding, not only in features such as orientation, color, and spatial frequency (Greenwood, Bex, & Dakin,, 2012; Greenwood & Parsons, 2020; Harrison & Bex, 2015; Poder & Wagemans, 2007; van den Berg, Roerdink, & Cornelissen, 2010) but also in objects such as letters (Freeman, Chakravarthi, & Pelli, 2012) and faces (Kalpadakis-Smith, Goffaux, & Greenwood,

2018). For example, Harrison and Bex (2015) used a population pooling model that takes a weighted combination of population responses to the target and flankers to account for both substitution and averaging errors. Recently, Shechter and Yashar (2021) compared various mixture models and demonstrated that crowding reflects sampling over a weighted sum of the represented features, as the outer flanker was more heavily weighted compared to the inner one. These findings are in accord with recent models that account for crowding as population coding with weighted summation within receptive fields (Dayan & Solomon, 2010).

Researchers have been seeking effective ways to relieve crowding. Several studies have demonstrated that cueing of a crowded target location reduces the crowding effects (Anton-Erxleben & Carrasco, 2013; Kewan-Khalalyly, Migó, & Yashar, 2022; Kewan-Khalalyly & Yashar, 2022; Talgar, Pelli, & Carrasco, 2004; Yeshurun & Carrasco, 1999), and modulating attentional allocation could affect inner–outer asymmetry (Chakravarthi, Rubruck, Kipling, & Clarke, 2021; Kewan-Khalalyly & Yashar, 2022; Kewan & Yashar, 2021; Petrov & Meleshkevich, 2011b). However, the role of attentional modulation has still been controversial, as some studies have reported that it has little or even no effect on crowding (Huckauf & Heller, 2002; Nazir, 1992; Scolari, Kohnen, Barton, & Awh, 2007; Wilkinson, Wilson, & Ellemberg, 1997). In contrast, recent studies have demonstrated that crowding can be reduced by perceptual learning in typical and clinical populations (Chung, 2007; Chung, Li, & Levi, 2012; Huckauf & Nazir, 2007; Hussain, Webb, Astle, & McGraw, 2012; Malania, Pawellek, Plank, & Greenlee, 2020; Maniglia, Pavan, Cuturi, Campana, Sato, & Casco, 2011; Sun, Chung, & Tjan, 2010; Xiong, Yu, & Zhang, 2015; Yashar, Chen, & Carrasco, 2015; Zhu, Fan, & Fang, 2016). For example, Chung (2007) trained observers to identify the middle flanked letters in trigrams and showed that training strongly reduced the extent of crowding. Recently, we trained observers with a partial report task, in which the observers reported the central target letter of a three-letter string presented in the visual periphery, or a whole report task, in which the observers reported all three letters in order. We found that training indeed reduced crowding but did not reduce target misplacement errors or flanker substitution errors when these errors are normalized by the corresponding recognition errors. This disassociation between target recognition and flanker substitution errors supports the view that flanker substitution may be more likely a byproduct due to response bias rather than a cause of crowding (Xiong et al., 2015).

Although previous studies have demonstrated a training-induced reduction of crowding, it is still unknown whether inner–outer asymmetry could be

reduced by training, whether the learning transfers to untrained conditions, for how long the learning persists, and what mechanisms underlie this learning. In the present study, we first investigated the contribution of inner and outer flankers to the pattern of crowding errors in a radial Gabor orientation crowding display with an orientation identification task (Experiment 1). Then we introduced perceptual training paradigms to evaluate their effects on crowding (Experiment 2). Moreover, we investigated whether the benefit would still be there 4 to 6 months after training. We hope our results provide a more detailed understanding of the mechanism of the inner–outer asymmetry in crowding.

Methods

Observers and apparatus

A total of 20 observers (mean $\pm$ *SD* age = 23.5 $\pm$ 4.4 years) with normal or corrected-to-normal vision participated in this study. Observers CYR, ZYW, and ZJY were coauthors and were experienced in psychophysical experiments. The others were new to psychophysical observations and were unaware of the purposes of the study. Written informed consent was obtained from all observers before data collection. This study was approved by the Peking University Institution Review Board.

The stimuli were generated with Psychtoolbox-3 (Pelli, 1997) and MATLAB (MathWorks, Natick, MA) and presented on a 21-inch G520 color monitor (Sony Corporation, Tokyo, Japan) with a resolution of 2048 $\times$ 1536 pixels and a 75-Hz refresh rate. The monitor was calibrated to give a mean luminance of 50 cd/m^2. Observers viewed stimuli binocularly from a distance of 80 cm, with head movements minimized using a head and chin rest. Responses were given via a keypad. An EyeLink 1000 eye tracker (SR Research, Kanata, Ontario, Canada) was used to monitor eye movements. Trials with eye position deviations beyond 2° relative to the fixation dot were aborted and replaced by a new randomly generated trial.

Stimuli and procedures

In all experiments, the stimuli were a Gabor patch, a sinusoidal grating vignette by a Gaussian envelope with a spatial frequency of 5 cycles/degree and fixed contrast at 47%, in which $\sim$1.5 periods of the sinusoidal pattern were visible. The center-to-center separation of the target and flankers was 2.25°. Observers were required

to maintain fixation on a circle with a 0.3° diameter and report the target orientation (clockwise [CW] or counterclockwise [CCW] from the vertical orientation). The target was presented at 7.5° eccentricity on the horizontal meridian of either left or right visual field (Figure 1A). The location of the visual field was randomly selected for each observer and was fixed across the test. Stimuli were presented for 425 ms after fixation (400 ms) and the next trial started 400 ms later than the response.

All 20 observers participated in Experiment 1 (Test 1) (Figure 1B). In Experiment 1, the target had nine orientations (0°, $\pm$3°, $\pm$6°, $\pm$9°, $\pm$12°) and the flanker had six orientations (0°, $\pm$30°, $\pm$60°, $-$90°). There were three conditions: one unflanked condition (target without flanker) and two flanked conditions (target with an inner flanker or an outer flanker) (Figure 1A). In the unflanked condition, each block had six repeat trials per target orientation, giving 54 trials per block. In the flanked conditions, the target was presented either with an inner flanker or with an outer flanker in a separate block. Each block had two repeat trials per combination of orientation between target and flanker stimuli, giving 108 trials per block. Unflanked blocks were repeated four times, and flanked blocks were repeated 12 times each for inner and outer flankers. All 28 blocks were run following a permuted table to give a total of 2808 trials per observer, completed in two sessions. Each session consisted of 14 blocks and lasted for 1 hour. No feedback was provided. Before collecting the data, all observers were trained with each condition for one block to make sure they fully understood the test. In the experimental blocks, detailed instructions were displayed on the screen to remind the observers which stimulus to report on. The observer initiated the experiment with a key press when they understood the current task.

Because of time constraints, only nine observers from Experiment 1 were able to participate in Experiment 2 within 2 weeks. These observers continued to perform a training task for four sessions (Figure 1B). The training task was the flanked condition with an outer flanker as in Test 1. The target had nine orientations (0°, $\pm$3°, $\pm$6°, $\pm$9°, $\pm$12°) and the outer flanker stimuli had six orientations (0°, $\pm$30°, $\pm$60°, $-$90°). Each block had two repeat trials per combination of orientation between target and flanker stimuli, giving 108 trials per block. Each training session consisted of 10 blocks (1080 trials in total) and no feedback was provided. The observers were tested again (Test 2) after four sessions of training to evaluate the training effects. Test 2 was the same as Test 1. To evaluate the retention effects, six observers of Experiment 2 were called back after 4 to 6 months (mean $\pm$ *SD* = 4.8 $\pm$ 0.4 months) to participate in a retention test. The retention test was the same as Test 1/Test 2.
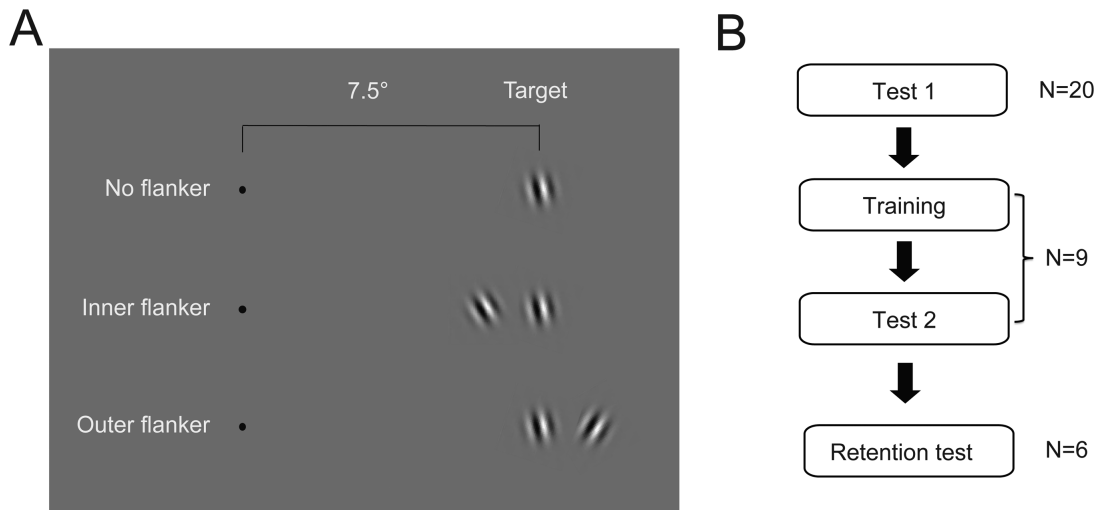
Figure 1. Stimuli and experimental design. (**A**) An example of stimuli. Observers were required to maintain fixation dot and report the orientation of the Gabor target (7.5° eccentricity) that was present alone or flanked by an inner or outer Gabor along the horizontal meridian. (**B**) Study design: All 20 observers participated in Test 1, and nine observers continued to perform a training task for four sessions; they were tested again (Test 2) after training. Six observers were called back and participated in a retention test after 4 to 6 months.

Analyses

In Experiments 1 and 2, psychometric functions were fit to data as a cumulative Gaussian function with three free parameters: midpoint or point of subjective equality (PSE) at 50%, slope, and lapse rate. Functions were fit separately for each observer and each flanker condition. Shifts in the midpoint were taken as changes in appearance (i.e., assimilation vs. repulsion errors). Thresholds were taken as the difference in the orientation required to shift performance from the midpoint to 75% CW responses, with a crowding index (or threshold elevation) obtained by dividing flanked thresholds by unflanked thresholds. The Greenhouse–Geisser correction was used when Mauchly's test of sphericity had been violated (Greenhouse & Geisser, 1959).

Models

Data in Experiments 1 and 2 were fitted with a population coding model, which was similar to the prior models (Greenwood et al., 2012). This approach regarded crowding as the weighted combination of population responses to the target and flanker stimuli, which have previously been found to reproduce the systematic error that arise (Harrison & Bex, 2015). To simulate the crowding of orientation, a population coding model with four free parameters was conducted.

We first calculated the probabilistic effects of crowding to determine its strength of crowding. The

probabilistic effect of orientation crowding (p_θ) is defined as

$$p_\theta = \alpha e^{\frac{-(\delta_\theta - \mu)^2}{2\sigma_c}}$$

where δ_θ represents the orientation difference between target and flanker stimuli, σ_c sets the width of the tuning function (the first free parameter), α sets the peak of the tuning function (the second free parameter), and μ was centered on 0°.

If crowding occurs, the perceived target orientation (t_c) with a weighted average of the orientation of target and flanker stimuli is defined as

$$t_c = t_v w_t + f_v w_f$$

where t_v and f_v are the veridical orientation of target and flanker stimuli, w_t is the weight of the target value in the average (the third free parameter), and w_f is the flanker weight (equal to $1 - w_t$).

The probability of a CW response (p_{cw}) for each combined of target and flanker orientation is calculated as

$$p_{cw} = \frac{1}{\sigma_t \sqrt{2\pi}} \int_{-\infty}^{x} e^{\frac{-(x-\mu)^2}{2\sigma_t^2}} dx$$

where σ_t sets the width of the tuning function (the fourth free parameter) and x is 0. If crowding occurred, the μ was centered on t_c; if crowding did not occur, then μ was centered on t_v. The best-fitting parameters were selected using maximum likelihood estimation.

Results

Experiment 1: Dissociate distinct crowded errors in inner–outer asymmetry

In Experiment 1, 20 observers were asked to report the orientation of a target Gabor (CW or CCW from the vertical orientation) presented either isolated or with an inner flanker or an outer flanker. For each observer, psychometric functions were fit separately for each condition to estimate the PSE (the 50% midpoint) and the thresholds (the difference from 50% to 75% CW responses). Example data are shown in Figures 2A to 2C. When unflanked, the judgments of target orientation (Figure 2C, black curve) transitioned rapidly from predominantly CCW to CW when the target orientation was around 0°. The psychometric function shows low bias in the PSE, with the steep slope indicating a low threshold. Psychometric functions of target performance with different flanker orientations were presented for the outer flanker condition and inner
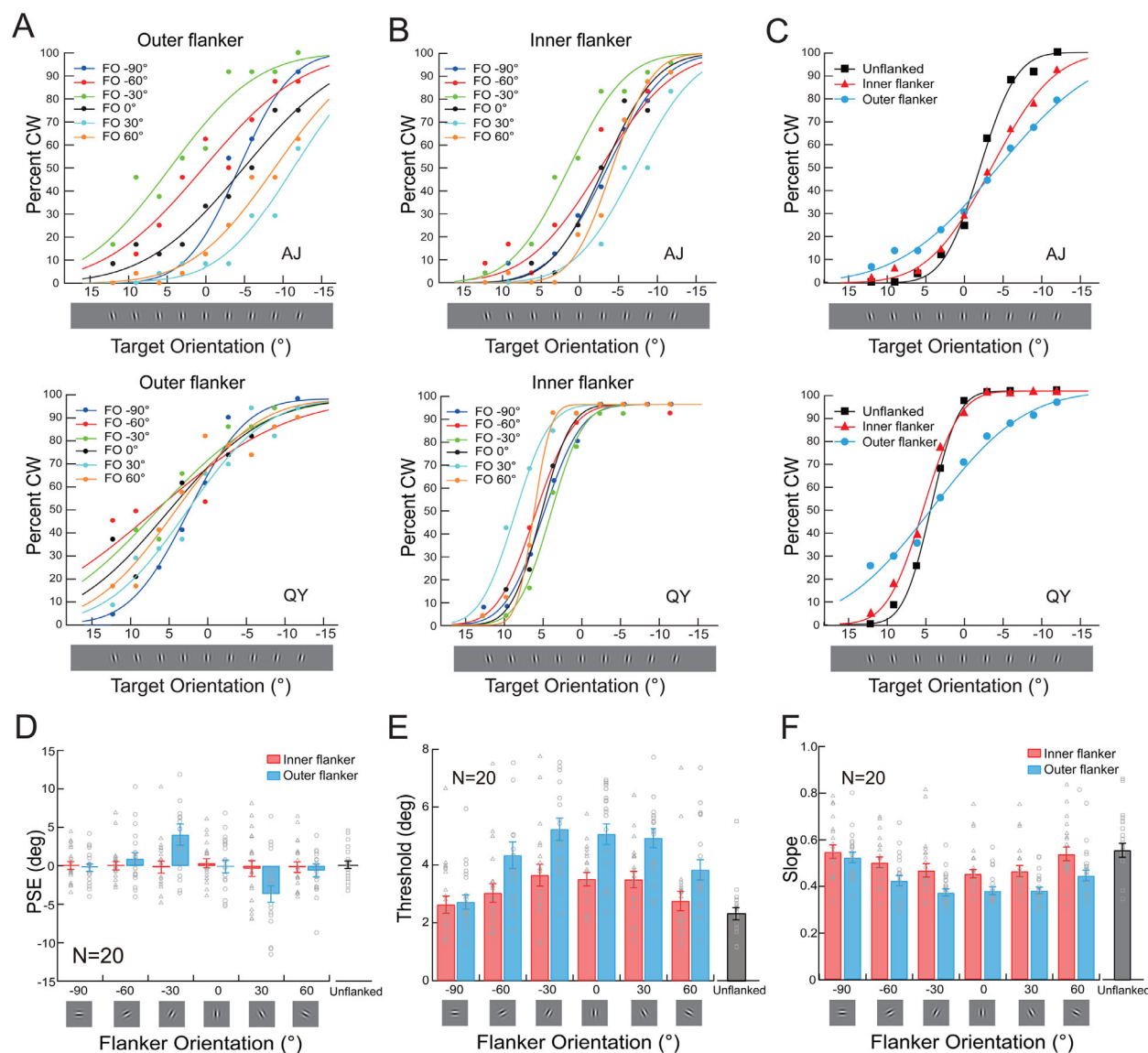

Figure 2. The crowding effect of target orientation identification (Experiment 1). **(A–C)** Psychometric functions with the proportion of CW responses plotted as a function of target orientation for two example observers (top, observer AJ; bottom, observer QY). Data are shown for a target with an outer flanker **(A)** or an inner flanker **(B)** for different flanker orientations. **(C)** The performance of target orientation identification with six flanker orientations was averaged. Data are shown for an unflanked target (black curve), a target with an inner flanker (red curve), and a target with an outer flanker (blue curve). **(D–F)** The PSE values, thresholds, and slopes for the unflanked (black bar), the inner flanker (red bar), and the outer flanker (blue bar) conditions were averaged over all observers across different flanker orientations. The gray symbols represent data for each observer. Error bars indicate 1 *SEM*.

flanker condition (Figures 2A and 2B). In the outer flanker condition (Figure 2A), the target judgments with a −90° flanker (dark blue point) transitioned more rapidly and showed low bias in the PSE with a steep slope. In contrast, a −30° flanker (light green) induced a strong bias toward a CW response, causing a leftward shift of the psychometric function in addition to the shallower slope. The opposite bias arose with a 30° flanker (light blue). The data with the inner flanker (Figure 2B) show the same pattern but with a weaker bias. To evaluate the general crowding effect, the performance of target orientation identification with six flanker orientations (0°, ±30°, ±60°, −90°) was averaged. The results indicate that the outer flanker (Figure 2C, blue circles and curve) induced stronger impairments in target performance than the inner flanker did (Figure 2C, red triangles and curve), as shallower psychometric functions were observed in the outer flanker condition. To see the bias in the PSE more specifically, the mean and individual PSE values were plotted as a function of flanker orientation for flanked conditions, and the mean and individual PSE values of the unflanked condition are provided in Figure 2D.

The mean thresholds of three conditions (unflanked, inner flanker, and outer flanker) are plotted as a function of flanker orientation in Figure 2E. The mean threshold of the unflanked condition (2.29° ± 0.93°) was plotted as a black bar. The thresholds of flanked conditions were entered into a two-way analysis of variance (ANOVA) with flanker condition (inner flanker vs. outer flanker) and flanker orientation (0°, ±30°, ±60°, −90°) as the repeated measures. A significant difference in threshold between two different flanked conditions was found, $F(1, 19) = 28.12$, $p < 0.01$, $\eta_p^2 = 0.60$, with a lower threshold with the inner flanker (3.50° ± 1.25°) than with the outer flanker (4.82° ± 1.57°). A significant interaction effect between flanker condition and flanker orientation was also found, $F(5, 95) = 4.80$, $p < 0.01$, $\eta_p^2 = 0.20$. Pairwise comparisons indicated that this interaction was mainly due to the significant difference in different flanker orientations between inner and outer flanker conditions ($p < 0.05$ for 0°, ±30°, ±60°).

The slopes of the psychometric functions for flanked conditions were also entered into a two-way ANOVA with flanker condition (inner flanker vs. outer flanker) and flanker orientation (0°, ±30°, ±60°, −90°) as the repeated measures. A significant difference in slope between two different flanked conditions was found, $F(1, 19) = 27.35$, $p < 0.01$, $\eta_p^2 = 0.59$, with a steeper slope with the inner flanker (0.45 ± 0.10) than with the outer flanker (0.38 ± 0.09) (Figure 2F).

To quantify the strength of the inner–outer asymmetry, we calculated the ratio of the threshold with the outer flanker to that with the inner flanker and adopted the criteria for inner–outer asymmetry from a recent study (Chakravarthi et al., 2021). Our results showed that the ratio was significantly greater than 1 (mean = 1.46; $SD = 0.56$; $t = 3.61$; $df = 19$; $p < 0.01$, one-sample t-test), indicating a significant inner–outer asymmetry.

The mean difference of PSE values (the difference between flanked and unflanked conditions) are plotted as a function of flanker orientation in Figure 3A. Two example datasets are shown in Figures 3B and 3C. A population coding model was used to fit these results (curves in Figures 3A to 3C). The PSE difference was then entered into a two-way ANOVA with flanker condition (inner flanker vs. outer flanker) and flanker orientation (0°, ±30°, ±60°, −90°) as the repeated measures. A significant main effect of flanker orientation was found, $F(5, 95) = 4.88$, $p < 0.01$, $\eta_p^2 = 0.20$. We also found a significant interaction effect of flanker condition and flanker orientation, $F(1.63, 30.88) = 14.07$, $p < 0.01$, $\eta_p^2 = 0.43$, in the PSE difference. When the flanker was presented outer (Figure 3A, blue circles), the PSE difference changed significantly with the −30° flanker and 30° flanker (all $p < 0.05$), indicating systematic crowded errors (assimilative errors, biased predominantly toward the flanker identities). When the flanker was presented inner (Figure 3A, red triangles), little changes in PSE difference were found (all $p > 0.05$). Examining these findings more closely, we can see that the observers showed two different systematic crowding errors. Some of them showed the assimilative errors (Figure 3B, red triangles), such that flanker orientation moving toward CCW induced a positive PSE difference, indicating an increase in CCW response. In contrast, some others showed repulsive errors (Figure 3C, red triangles), such that flanker orientation moving toward CCW induced a negative PSE difference. We conducted a paired-sample t-test to examine the difference of w_f, which represents the weights of the flanker value of the inner flanker or the outer flanker. The results showed that the flanker weights in the outer flanker condition were significantly higher than those in the inner flanker condition (Figure 3D), $t = −4.08$, $df = 19$, $p < 0.01$, suggesting that the observers tended to rely more on the flanker orientation when identifying target orientation with an outer flanker.

We found individual differences in the strength of inner–outer asymmetry, as not all observers showed high asymmetry (three out of 20 observers showed no inner–outer asymmetry) and crowding errors. Because Test 1 was completed in two separate sessions, we were able to compare the threshold, crowding index, slopes of the psychometric functions, and PSE difference between the first session and the second session of Test 1. These comparisons provide information about the reliability of observers' responses. Three-way ANOVA was conducted with flanker condition (inner flanker vs. outer flanker), flanker orientation (0°, ±30°, ±60°, −90°), and test time (first session vs. second session) as
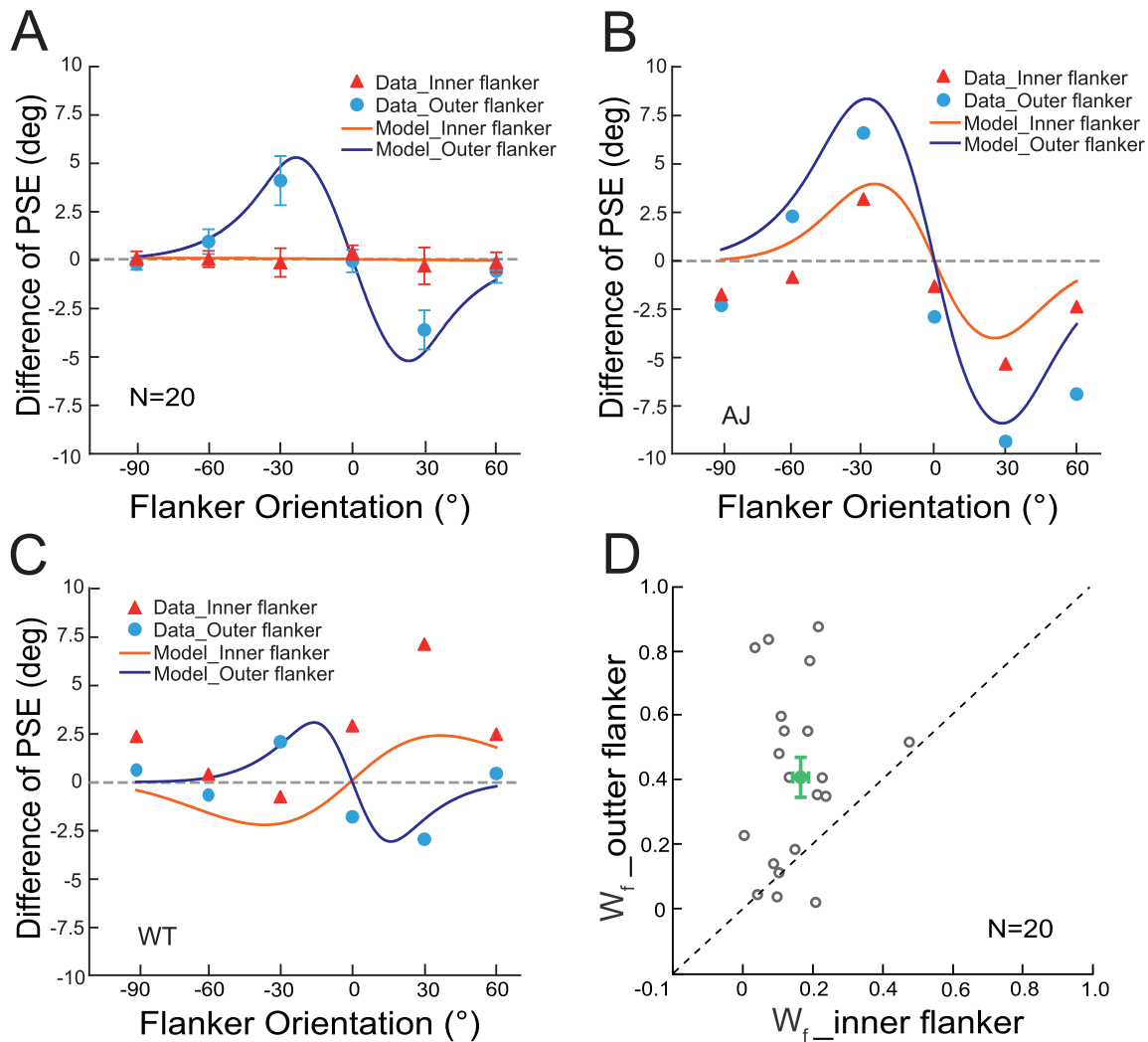
Figure 3. PSE difference and model fit results (Experiment 1). (**A–C**) PSE difference for the outer flanker condition (blue circles) and the inner flanker condition (red triangles) plotted as a function of flanker orientation. The output of a population coding model for the outer flanker condition (dark blue curve) and the inner flanker condition (orange curve) is shown. (**A**) Average data and the mean output of a population coding model ($R^2 = 0.97$ for outer flanker condition; $R^2 = 0.96$ for inner flanker condition). (**B**, **C**) Two example data ($R^2 = 0.74$ and $R^2 = 0.91$ for the outer flanker condition; $R^2 = 0.79$ and $R^2 = 0.74$ for the inner flanker condition). (**D**) The flanker weight for the outer flanker is plotted as a function of the flanker weight for the inner flanker. The green solid circle represents the averaging data, and the gray hollow symbols represent data for each observer. Error bars indicate 1 *SEM*.

the repeated measures. No significant main effect was found on test time in the threshold ($p = 0.16$), crowding index ($p = 0.28$), slope ($p = 0.33$), or PSE difference ($p = 0.42$). These results indicate that the observers' responses were reliable for similar target/flanker combinations across sessions. We further reanalyzed the fitted w_f for the first session and second session of Test 1, and a two-way ANOVA was conducted with flanker condition (inner flanker vs. outer flanker) and test time (first session vs. second session) as the repeated measures. No significant main effect on test time ($p = 0.31$) and no significant interaction effect ($p = 0.95$) were found for w_f.

To rule out the influence of the visual field on the performance, we compared the performance of the observers who were tested at different visual fields (left visual field vs. right visual field) in Test 1. Their threshold, crowding index, the slopes of the psychometric functions, and PSE difference were evaluated in three two-way ANOVAs with flanker condition (inner flanker vs. outer flanker) and flanker orientation (0°, ±30°, ±60°, −90°) as the repeated measures. No significant effect was found on the visual field in the threshold ($p = 0.73$), crowding index ($p = 0.19$), slope ($p = 0.92$), or PSE difference ($p = 0.73$), indicating no difference in the performance
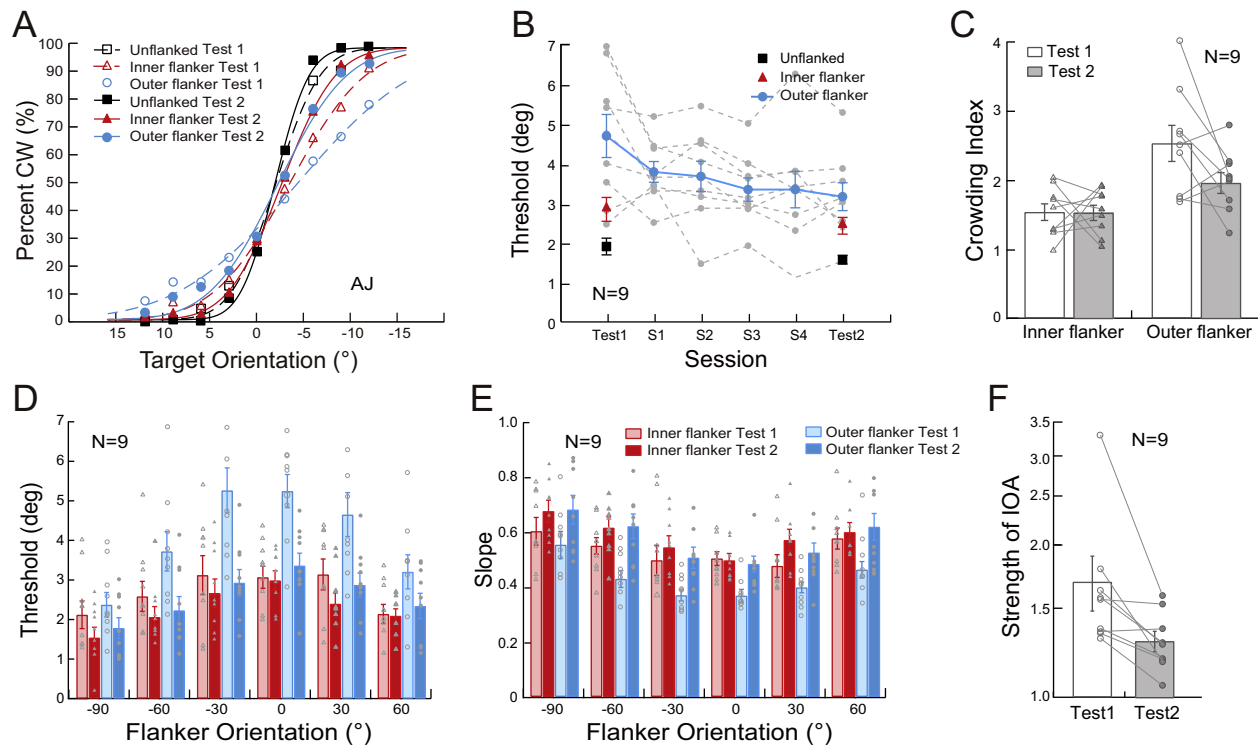
Figure 4. The effect of perceptual learning on inner–outer asymmetry (Experiment 2). (**A**) Psychometric functions for example data with the proportion of CW responses plotted as a function of target orientation. Data are shown for the unflanked condition (black squares), inner flanker condition (red triangles, untrained condition), and outer flanker condition (blue circles, trained condition) for Test 1 (dashed lines) and Test 2 (solid lines). (**B**) The mean and individual learning curve of thresholds through all sessions. The gray symbols indicate individuals' data. (**C**) The crowding index of the flanked conditions averaged over all observers for Test 1 and Test 2. The gray symbols indicate individuals' data. (**D**, **E**) The threshold and slope for the flanked condition averaged over all observers across different flanker orientations for Test 1 and Test 2. The gray triangles and circles represent data for each observer for a target with an inner flanker and a target with an outer flanker, respectively (open symbols for Test 1 and filled symbols for Test 2). (**F**) The strength of the inner–outer asymmetry (IOA) averaged over all observers at Test 1 and Test 2. The gray symbols indicate individuals' data. Y-axis is in logarithmic scale. Error bars indicate 1 *SEM*.

Experiment 2: The impact of training on the inner–outer asymmetry in crowding

In Experiment 1, a strong effect of inner–outer asymmetry was shown; however, it is unclear whether this asymmetry could be reduced by perceptual learning. Nine observers from Experiment 1 (Test 1) participated in Experiment 2. The observers were trained with a crowding task for four sessions. The training task was the flanked condition with an outer flanker as in Test 1. During training, each observer completed 10 flanked blocks (108 trials/block) with an outer flanker per session. The observers were retested (Test 2) after training to evaluate the learning effects.

Psychometric functions were fit separately for each observer and each flanker condition to evaluate threshold and PSE for Test 1 and Test 2. Example data

are shown in Figure 4A. The psychometric function for the trained outer flanker condition (blue curve) became steeper for Test 2, suggesting a potential change of threshold and PSE through training. For the untrained inner flanker condition (red curve) and unflanked condition (black curve), little change was found in the PSE and the slopes of the psychometric functions between Test 1 and Test 2.

After training, the mean threshold for the trained outer flanker condition was decreased by 32.23% (Figure 4B), from 4.72° ± 1.62° to 3.20° ± 1.04°, and the untrained inner flanked condition was changed by 14.22% (Figure 4B), from 2.88° ± 0.89° to 2.47° ± 0.64°, suggesting that learning was specific to the trained condition. The threshold changes as a function of flanker orientation are shown in Figure 4D. We conducted a two-way ANOVA with flanker orientation (0°, ±30°, ±60°, −90°) and test time (Test 1, four training sessions, Test 2) as the repeated measures to examine the threshold in the outer flanker condition to see the learning effect. We found a significant
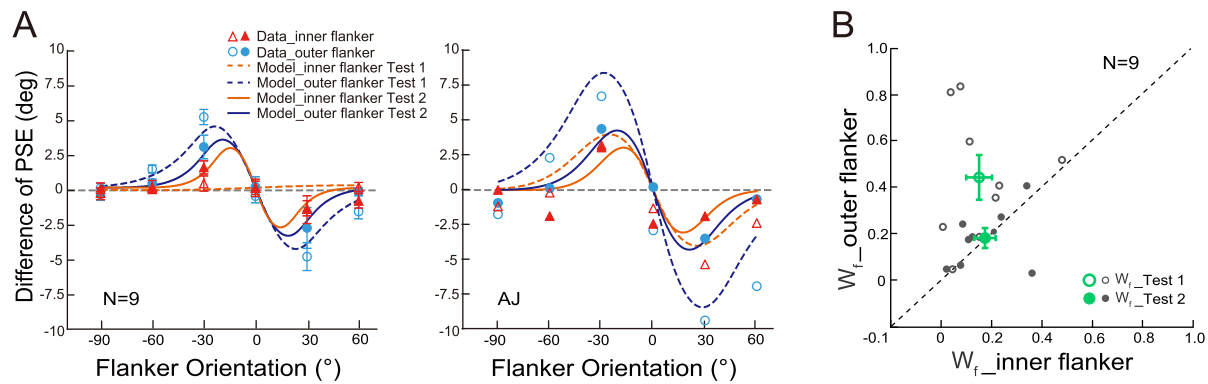
Figure 5. The effect of perceptual learning on PSE difference and model fit results (Experiment 2). (**A**) Left: The mean difference in PSE values averaged over all observers across different flanker orientations for Test 1 and Test 2, and the output of a population coding model for the outer flanker condition (dark blue curve) and the inner flanker condition (orange curve) for Test 1 (dashed lines) and Test 2 (solid lines). $R^2 = 0.97$ and $R^2 = 0.98$ for the outer flanker condition and $R^2 = 0.97$ and $R^2 = 0.98$ for the inner flanker condition for Test 1 and Test 2, respectively. Right: Example data, where $R^2 = 0.73$ and $R^2 = 0.89$ for the outer flanker condition and $R^2 = 0.79$ and $R^2 = 0.85$ for the inner flanker condition for Test 1 and Test 2, respectively. (**B**) The flanker weight in the outer flanker condition was plotted as a function of the flanker weight in the inner flanker condition for Test 1 (open circle) and Test 2 (filled circle). Error bars indicate 1 *SEM*.

main effect on test time, $F(5, 40) = 12.13$, $p < 0.01$, $\eta_p^2 = 0.60$. A significant interaction effect between flanker orientation and test time was also found, $F(25, 200) = 1.88$, $p < 0.05$, $\eta_p^2 = 0.19$. Pairwise comparisons indicated significant changes between the first and second training sessions and Test 2 ($p < 0.05$), suggesting that significant learning occurred during the first few sessions.

The slopes of the psychometric functions for the flanked conditions were compared to a three-way ANOVA with flanker condition (inner flanker vs. outer flanker), flanker orientation (0°, ±30°, ±60°, −90°), and test time (Test 1 vs. Test 2) as the repeated measures. We found significant main effect of flanker condition, $F(1, 8) = 38.26$, $p < 0.01$, $\eta_p^2 = 0.83$; flanker orientation, $F(5, 40) = 20.94$, $p < 0.01$, $\eta_p^2 = 0.72$; and test time, $F(1, 8) = 5.33$, $p < 0.05$, $\eta_p^2 = 0.40$. We also found a significant interaction effect between the flanker condition and test time, $F(1, 8) = 12.13$, $p < 0.01$, $\eta_p^2 = 0.60$, which was mainly due to significant changes between Test 1 and Test 2 ($p < 0.05$) in the trained outer flanker condition (Figure 4E).

We quantified crowding effects with a crowding index, which was defined as the ratio of the flanked condition to the unflanked condition (Figure 4C). The crowding index was compared to a three-way ANOVA with flanker condition (inner flanker vs. outer flanker), flanker orientation (0°, ±30°, ±60°, −90°), and test time (Test 1 vs. Test 2) as the repeated measures. We found a significant main effect of flanker condition, $F(1, 8) = 51.83$, $p < 0.01$, $\eta_p^2 = 0.87$, and flanker orientation, $F(5, 40) = 19.71$, $p < 0.01$, $\eta_p^2 = 0.71$. A significant interaction effect between the flanker condition and time was also found, $F(1, 8) = 23.89$,

$p < 0.01$, $\eta_p^2 = 0.75$. Pairwise comparisons indicated that this interaction was mainly due to significant changes in outer flanker conditions between Test 1 and Test 2 ($p < 0.05$), suggesting that the reduction of crowding was specific to the trained outer flanker condition.

To quantify the improvement of strength of inner–outer asymmetry, we calculated the improvement of the ratio of the threshold with the outer flanker to that with the inner flanker for Test 1 and Test 2. The strength of the inner–outer asymmetry was decreased by 18.35% (Figure 4F), from 1.69 ± 0.63 to 1.29 ± 0.17, which was significantly greater than 0 (one-sample *t*-test, $t = 2.65$, $df = 8$, $p < 0.05$). There were individual variabilities, as indicated by the different improvements across observers. One observer showed no improvement in the strength of inner–outer asymmetry (improvement: −1.4%), and one even showed retrogression (improvement: −13.6%); the other seven observers showed improvement ranging from 12.0% to 58.8%.

We also examined the changes of PSE difference (difference between flanked and unflanked condition) by conducting a three-way ANOVA with flanker condition (inner flanker vs. outer flanker), flanker orientation (0°, ±30°, ±60°, −90°), and test time (Test 1 vs. Test 2) as the repeated measures. We found a significant main effect of flanker orientation, $F(1.95, 15.58) = 10.18$, $p < 0.01$, $\eta_p^2 = 0.56$. A significant interaction effect among flanker condition, flanker orientation, and test time was also found, $F(1.49, 11.89) = 3.89$, $p < 0.01$, $\eta_p^2 = 0.33$. Pairwise comparisons indicated that this interaction was mainly due to the significant difference in different flanker orientations between inner and outer
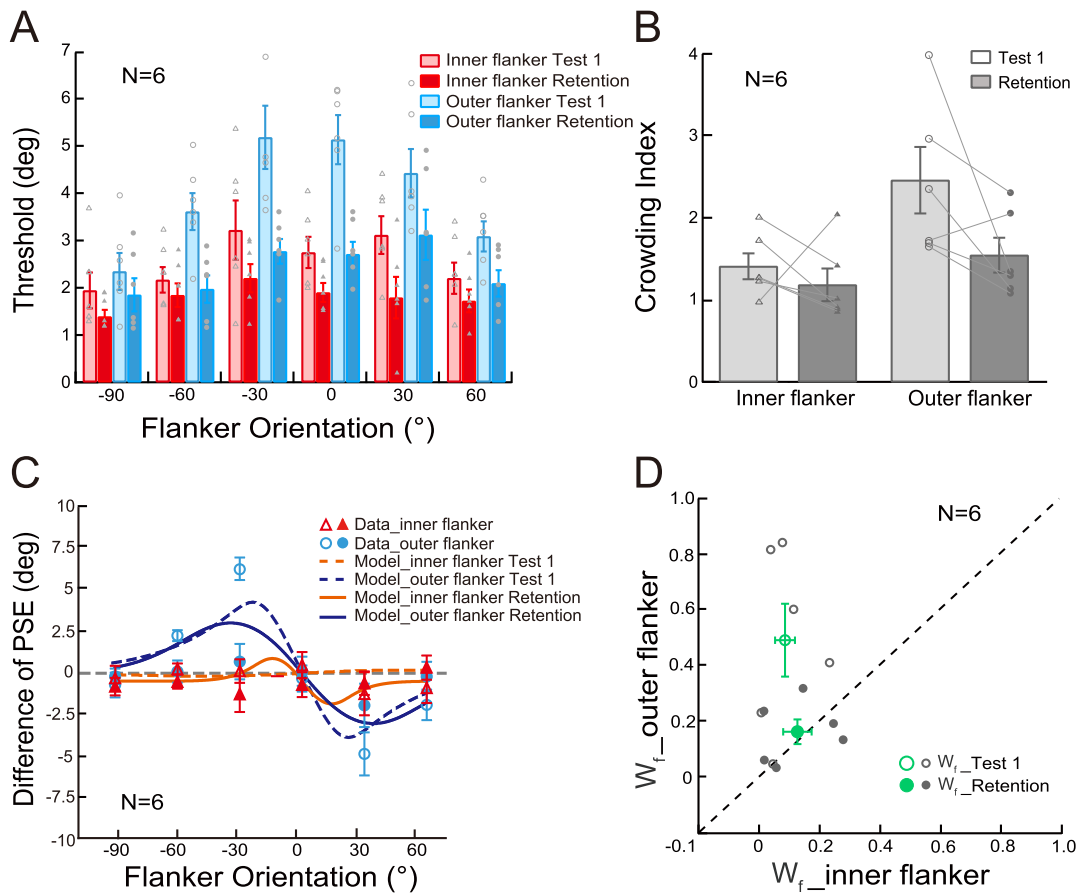
Figure 6. Retention effect of perceptual training (Experiment 2). (**A**) The threshold of flanked condition averaged over six observers across different flanker orientations for Test 1 and the retention test. The gray triangles and circles represent data for each observer for a target with an inner flanker and a target with an outer flanker, respectively (open symbols for Test 1 and filled symbols for the retention test). (**B**) The average crowding index of the flanked condition for Test 1 and for the retention test. (**C**) The mean PSE difference across different flanker orientations for Test 1 and the retention test, showing the output of a population coding model for the outer flanker condition (dark blue curve) and the inner flanker condition (orange curve) for Test 1 (dashed lines) and retention test (solid lines). $R^2 = 0.97$ and $R^2 = 0.94$ for the outer flanker condition and $R^2 = 0.96$ and $R^2 = 0.96$ for the inner flanker condition for Test 1 and the retention test, respectively. (**D**) The flanker weight for the outer flanker was plotted as a function of the flanker weight for the inner flanker for Test 1 (open circle) and the retention test (filled circle). Error bars indicate 1 *SEM*.

flanker conditions ($p < 0.05$ on ±30°) for Test 1 and Test 2.

The fitting results of a population coding model for Test 1 and Test 2 were plotted in Figure 5A. We conducted a two-way ANOVA with flanker condition (inner flanker vs. outer flanker) and test time (Test 1 vs. Test 2) as the repeated measures to examine the change of w_f before and after training. We found significant main effect of flanker condition ($F(1, 8) = 5.57$, $p < 0.05$, $\eta_p^2 = 0.41$) and test time ($F(1, 8) = 6.87$, $p < 0.05$, $\eta_p^2 = 0.46$). A significant interaction effect among flanker condition and test time were also found ($F(1, 8) = 6.46$, $p < 0.05$, $\eta_p^2 = 0.45$). Pairwise comparisons indicated that this interaction was mainly due to the significant reduction in w_f in the outer flanker condition between Test 1 and Test 2 ($p < 0.05$, Figure 5B), suggesting that the observers relied less

on the flanker orientation when identifying target orientation with an outer flanker after training.

To examine the long-term effect of training on inner–outer in crowding, six observers were retested 4∼6 months after they finished training. The threshold, slope of the psychometric function, crowding index, and PSE difference were compared between Test 1 and the retention test to four three-way ANOVA with flanker condition (inner flanker vs. outer flanker), flanker orientation (0°, ±30°, ±60°, −90°), and test time (Test 1 vs. the retention test) as the repeated measures. Significant interaction effects were found between flanker condition and test time (Test 1 vs. retention test) in the threshold (Figure 6A), $F(1, 5) = 24.72$, $p < 0.01$, $\eta_p^2 = 0.83$; slope, $F(1, 5) = 29.51$, $p < 0.01$, $\eta_p^2 = 0.86$; and crowding index (Figure 6B), $F(1, 5) = 11.29$, $p < 0.05$, $\eta_p^2 = 0.69$. No such effect was found in PSE

difference (Figure 6C). Pairwise comparisons indicated that the threshold, slope, and crowding index showed significant changes between Test 1 and the retention test for the outer flanker condition (all $p < 0.05$). We also conducted a two-way ANOVA with flanker condition (inner flanker vs. outer flanker) and test time (Test 1 vs. retention test) as the repeated measures to examine the change of w_f. We found a significant main effect of flanker condition, $F(1, 5) = 6.97$, $p < 0.05$, $\eta_p^2 = 0.58$, and test time, $F(1, 5) = 7.13$, $p < 0.05$, $\eta_p^2 = 0.59$. A significant interaction effect among flanker condition and test time was also found, $F(1, 5) = 8.49$, $p < 0.05$, $\eta_p^2 = 0.63$. Pairwise comparisons indicated a significant reduction in the weight of flanker values in the outer flanked condition between Test 1 and the retention test ($p < 0.05$) (Figure 6D). These results indicate that the reduction of crowding through training is persistent for 4 to 6 months.

Discussion

By investigating different systematic errors of inner–outer asymmetry in crowding, we showed that outer-flanker conditions induced a strong crowding effect, accompanied by stronger assimilative errors for the outer flanker for similar target/flanker elements. In contrast, the inner-flanker condition exhibited weak crowding, and no similar patterns of crowding errors were shown. A population coding model showed that the flanker weights in the outer flanker condition were significantly higher than that in the inner flanker condition. Moreover, we found that four sessions of training reduced inner–outer asymmetry and reduced flanker weights to the outer flanker. The learning effects were retained over 4 to 6 months. However, we also found individual differences in the appearance of crowding errors, the strength of inner–outer asymmetry, and the learning effects.

We replicated inner–outer asymmetry in the identification of Gabor patch orientation (Petrov & Meleshkevich, 2011a; Petrov & Meleshkevich, 2011b; Petrov et al., 2007; Shechter & Yashar, 2021). Our results are consistent with previous studies that demonstrated systematical errors biased by the appearance of the flanker element in the perceived orientation of a crowded target (Ester et al., 2014; Greenwood et al., 2009; Harrison & Bex, 2015), and the outer flankers dominate appearance more than the inner ones under crowding (Shechter & Yashar, 2021). Using a letter identification task, we recently showed that different crowding mechanisms may be responsible for the asymmetric crowding effects by inner and outer flankers (Zhang, Zhang,& Yu, 2018). That is, outer-flanker crowding consists of target-flanker confusion in visual short-term memory, feature confusion, and lateral masking, whereas inner-flanker crowding includes lateral masking only. This difference might explain the inner–outer asymmetry in letter identification. However, whether this explanation is applicable to explaining the inner–outer asymmetry in orientation identification requires future studies.

Harrison and Bex (2015) developed a population pooling model that takes a weighted combination of population responses to the target and flankers to account for both substitution and averaging errors. They asked observers to match the orientation of a reference Landolt-C to that of a crowded target in the periphery and found that observers made errors predominantly matched either intermediate orientations between the target and flankers (averaging) with 45° target/flanker orientation differences or the orientation of the flankers (substitution) with 90° target/flanker differences. We used the population-coding model and showed the outer flanker is assigned a higher weight than the inner flanker. Our assimilative errors to the outer flanker with 30° target/flanker orientation differences are similar to their averaging errors, which were found when requiring observers to make a spatial judgment about a continuous property of the target, such as its orientation, direction, or relative position (Dakin, Cass, Greenwood, & Bex, 2010; Greenwood & Parsons, 2020; Harrison & Bex, 2015). On the other hand, feature substitutions that misreport a flanker element as a target were found in different features, such as orientation, color, and letters (Ester et al., 2014; Ester et al., 2015; Freeman et al., 2012; Nandy & Tjan, 2007; Strasburger & Malania, 2013; Yashar, Wu, Chen, & Carrasco, 2019; Zhang et al., 2012). Flanker substitution might be a byproduct of crowding (Strasburger, 2005), as fewer flanker substitution errors were present in whole-report tasks than in partial-report tasks, and this difference can be mainly attributed to reduced outer-flanker substitution errors (Xiong et al., 2015), which was consistent with the response-bias explanation because the outer flanker is the most visible stimulus in a trigram.

We showed that training reduced the strength of crowding by 32.23%. These results are consistent with previous studies that showed that training relieves crowding by 30% to 88%, which depends on the training amount and training task (Chung, 2007; Huckauf & Nazir, 2007; Hussain et al., 2012; Maniglia et al., 2011; Plank, Lerner, Tuschewski, Pawellek, Malania, & Greenlee, 2021; Sun et al., 2010; Xiong et al., 2015; Yashar et al., 2015; Zhu et al., 2016). Our current study went beyond these findings by showing that perceptual learning reduced inner–outer asymmetry and the learning effects were retained over 4 to 6 months, accompanied by the reduced assigned weights to the outer flanker. Indeed, the remarkable reduction in crowding places a strong constraint on any model

for crowding. It has been argued that inner–outer asymmetry arises due to feature pooling where the weighted summation of available features is taken within receptive fields (Dayan & Solomon, 2010; Shechter & Yashar, 2021). It is speculated that training reduces inappropriate feature integration between target and flankers (Greenwood et al., 2009; Levi, Hariharan, & Klein, 2002; Pelli et al., 2004). In contrast, inner–outer asymmetry can also be attributed to the asymmetrical deployment of attention (Petrov & Meleshkevich, 2011b). An attentional bias toward the outer flanker can be argued to be equivalent to higher weights assigned to it. Training might help observers be more capable of focusing their attention on the target instead of dispersing their attention over the flankers. As it is, these two mechanisms are difficult to distinguish, although they implicitly point to different underlying mechanisms.

How does the brain implement the learning processes? Functional magnetic resonance imaging studies have revealed that training-induced reduction of crowding reflects a release of cortical suppression in multiple visual areas as early as V1 (Chen, Shin, Millin, Song, Kwon, & Tjan, 2019), and training-induced changes in the anisotropic shape of the crowding zone reflect changes in blood oxygen level-dependent (BOLD) signals in the early visual cortex (Malania et al., 2020). Using electroencephalogram frequency tagging to successfully dissociate the neural signals of the flankers and the target, Chicherov and Herzog (2015) demonstrated that the targets rather than the flankers were suppressed in crowding. The reduction of crowding in our results suggests its association with an enhanced signal-to-noise ratio of neural responses to the stimuli by refinement of neural population codes in the early visual cortex that represents the trained stimulus features. This assumption is in line with a recent electrophysiological study that recorded the neuronal populations in the monkey primary visual cortex (V1) and showed that spatial contextual effects in V1 limit the discriminability of visual features and can contribute substantively to crowding (Henry & Kohn, 2020). On the other hand, it is undeniable that crowding is associated with a top–down process that modulates early visual processing (Chen, He, Zhu, Zhou, Peng, Zhang, & Fang, 2014; Freeman, Sagi, & Driver, 2004; Han & Luo, 2019), as a delayed behavioral-relevant response in the high-level region was shown (Han & Luo, 2019). Further tests are needed to disentangle these learning effects in the brain.

One finding of our study is that learning was specific to the trained outer flanker condition, indicating the location specificity of learning. These results are consistent with previous studies that showed the partial location specificity of perceptual learning in crowding,

as learning was greater at the trained location than at the untrained location (Xiong et al., 2015; Yashar et al., 2015; Yeotikar, Khuu, Asper, & Suttle, 2013; Zhu et al., 2016). However, what we can learn from this partial location specificity requires further study. Many visual learning tasks are known to be at least partially specific to trained location and feature, which is often taken as evidence for training-induced neural plasticity in early visual areas such as V1 (Sagi, 2011). But, we and, more recently, other labs have demonstrated that "double training" could enable complete learning transfer to other untrained locations (Hung & Seitz, 2014; Pascucci, Mastropasqua, & Turatto, 2015; Wang, Cong, & Yu, 2013; Wang, Zhang, Klein, Levi, & Yu, 2012; Wang, Zhang, Klein, Levi, & Yu, 2014; Xiao, Zhang, Wang, Klein, Levi, & Yu, 2008; Zhang et al., 2010). These transfer results argue against the low-level explanation of visual perceptual learning by suggesting that learning may mostly occur in high-level brain areas. It is worth exploring whether "double training" can be effective in removing the location specificity in crowding-related perceptual learning, as the transfer effects could be used to infer the mechanisms underlying crowding and its learning.

Some limitations of this study could be addressed in future research. First, our results are limited to orientation errors of Gabor patches. Previous studies have shown crowding errors in other feature dimensions, such as orientation, color, spatial frequency, and motion (Greenwood & Parsons, 2020; Yashar et al., 2019) and different processes involved at feature and object levels (Manassi & Whitney, 2018). Therefore, further work is needed to determine whether the current findings apply to other feature dimensions and other types of stimulus, which would allow a clear distinction between the feature and object levels. Second, our results were consistent with prior reports of individual differences in the spatial extent of crowding (Kalpadakis-Smith, Tailor, Dahlmann-Noor, & Greenwood, 2022; Petrov & Meleshkevich, 2011a; Toet & Levi, 1992). Our results show that inner–outer asymmetry is not given for every observer. These results provide a challenge to the concern of whether inner–outer asymmetry can be considered a diagnostic marker of crowding. It is unclear whether this is specific to this task or is general to crowding. Indeed, it is reported that individual differences in crowding are correlated with population receptive field size in V2 (He, Wang, & Fang, 2019). Therefore, further work is needed to determine how the computational modeling and brain mechanisms are coordinated with behavior performance to account for individual differences in crowding.

Acknowledgments

Commercial relationships: none.
Corresponding author: Jun-Yun Zhang.
Email: zhangjunyun@pku.edu.cn.
Address: School of Psychological and Cognitive Sciences and Beijing Key Laboratory of Behavior and Mental Health, Peking University, Beijing, China.

References

Anton-Erxleben, K., & Carrasco, M. (2013). Attentional enhancement of spatial resolution: Linking behavioural and neurophysiological evidence. *Nature Reviews Neuroscience, 14*(3), 188–200, https://doi.org/10.1038/nrn3443.

Banks, W. P., Bachrach, K. M., & Larson, D. W. (1977). The asymmetry of lateral interference in visual letter identification. *Perception & Psychophysics, 22*(3), 232–240, https://doi.org/10.3758/bf03199684.

Bex, P. J., Dakin, S. C., & Simmers, A. J. (2003). The shape and size of crowding for moving targets. *Vision Research, 43*(27), 2895–2904, https://doi.org/10.1016/S0042-6989(03)00460-7.

Bouma, H. (1970). Interaction effects in parafoveal letter recognition. *Nature, 226*(5241), 177–178, https://doi.org/10.1038/226177a0.

Bouma, H. (1973). Visual interference in the parafoveal recognition of initial and final letters of words. *Vision Research, 13*(4), 767–782, https://doi.org/10.1016/0042-6989(73)90041-2.

Chakravarthi, R., Rubruck, J., Kipling, N., & Clarke, A. D. F. (2021). Characterizing the in-out asymmetry in visual crowding. *Journal of Vision, 21*(11):10, 1–14, https://doi.org/10.1167/jov.21.11.10.

Chaney, W., Fischer, J., & Whitney, D. (2014). The hierarchical sparse selection model of visual crowding. *Frontiers in Integrative Neuroscience, 8*, 73, https://doi.org/10.3389/fnint.2014.00073.

Chen, J., He, Y., Zhu, Z., Zhou, T., Peng, Y., Zhang, X., . . . Fang, F. (2014). Attention-dependent early cortical suppression contributes to crowding. *The Journal of Neuroscience, 34*(32), 10465–10474, https://doi.org/10.1523/jneurosci.1140-14.2014.

Chen, N., Shin, K., Millin, R., Song, Y., Kwon, M., & Tjan, B. S. (2019). Cortical reorganization of peripheral vision induced by simulated central vision loss. *The Journal of Neuroscience, 39*(18), 3529–3536, https://doi.org/10.1523/jneurosci.2126-18.2019.

Chicherov, V., & Herzog, M. H. (2015). Targets but not flankers are suppressed in crowding as revealed by EEG frequency tagging. *NeuroImage, 119*, 325–331, https://doi.org/10.1016/j.neuroimage.2015.06.047.

Chung, S. T. (2007). Learning to identify crowded letters: Does it improve reading speed? *Vision Research, 47*(25), 3150–3159, https://doi.org/10.1016/j.visres.2007.08.017.

Chung, S. T., Li, R. W., & Levi, D. M. (2012). Learning to identify near-acuity letters, either with or without flankers, results in improved letter size and spacing limits in adults with amblyopia. *PLoS One, 7*(4), e35829, https://doi.org/10.1371/journal.pone.0035829.

Dakin, S. C., Cass, J., Greenwood, J. A., & Bex, P. J. (2010). Probabilistic, positional averaging predicts object-level crowding effects with letter-like stimuli. *Journal of Vision, 10*(10):14, 1–16, https://doi.org/10.1167/10.10.14.

Dayan, P., & Solomon, J. A. (2010). Selective Bayes: Attentional load and crowding. *Vision Research, 50*(22), 2248–2260, https://doi.org/10.1016/j.visres.2010.04.014.

Ester, E. F., Klee, D., & Awh, E. (2014). Visual crowding cannot be wholly explained by feature pooling. *Journal of Experimental Psychology: Human Perception and Performance, 40*(3), 1022–1033, https://doi.org/10.1037/a0035377.

Ester, E. F., Zilber, E., & Serences, J. T. (2015). Substitution and pooling in visual crowding induced by similar and dissimilar distractors. *Journal of Vision, 15*(1):4, 1–12, https://doi.org/10.1167/15.1.4.

Farzin, F., Rivera, S. M., & Whitney, D. (2009). Holistic crowding of Mooney faces. *Journal of Vision, 9*(6):18, 1–15, https://doi.org/10.1167/9.6.18.

Freeman, E., Sagi, D., & Driver, J. (2004). Configuration-specific attentional modulation of flanker-target lateral interactions. *Perception, 33*(2), 181–194, https://doi.org/10.1068/p3481.

Freeman, J., Chakravarthi, R., & Pelli, D. G. (2012). Substitution and pooling in crowding. *Attention, Perception, & Psychophysics, 74*(2), 379–396, https://doi.org/10.3758/s13414-011-0229-0.

Freeman, J., & Simoncelli, E. P. (2011). Metamers of the ventral stream. *Nature Neuroscience, 14*(9), 1195–U1130, https://doi.org/10.1038/nn.2889.

Greenhouse, S. W., & Geisser, S. (1959). On methods in the analysis of profile data. *Psychometrika, 24*(2), 95–112, https://doi.org/10.1007/BF02289823.

Greenwood, J. A., Bex, P. J., & Dakin, S. C. (2009). Positional averaging explains crowding with letter-like stimuli. *Proceedings of the National Academy of Sciences, USA, 106*(31), 13130–13135, https://doi.org/10.1073/pnas.0901352106.

Greenwood, J. A., Bex, P. J., & Dakin, S. C. (2012). Crowding follows the binding of relative position and orientation. *Journal of Vision, 12*(3):18, 1–20, https://doi.org/10.1167/12.3.18.

Greenwood, J. A., & Parsons, M. J. (2020). Dissociable effects of visual crowding on the perception of color and motion. *Proceedings of the National Academy of Sciences, USA, 117*(14), 8196–8202, https://doi.org/10.1073/pnas.1909011117.

Han, Q., & Luo, H. (2019). Visual crowding involves delayed frontoparietal response and enhanced top-down modulation. *European Journal of Neuroscience, 50*(6), 2931–2941, https://doi.org/10.1111/ejn.14401.

Harrison, W. J., & Bex, P. J. (2015). A unifying model of orientation crowding in peripheral vision. *Current Biology, 25*(24), 3213–3219, https://doi.org/10.1016/j.cub.2015.10.052.

Harrison, W. J., Mattingley, J. B., & Remington, R. W. (2012). Pre-saccadic shifts of visual attention. *PLoS One, 7*(9), e45670, https://doi.org/10.1371/journal.pone.0045670.

He, D., Wang, Y., & Fang, F. (2019). The critical role of V2 population receptive fields in visual orientation crowding. *Current Biology, 29*(13), 2229–2236.e3, https://doi.org/10.1016/j.cub.2019.05.068.

He, S., Cavanagh, P., & Intriligator, J. (1996). Attentional resolution and the locus of visual awareness. *Nature, 383*(6598), 334–337, https://doi.org/10.1038/383334a0.

Henry, C. A., & Kohn, A. (2020). Spatial contextual effects in primary visual cortex limit feature representation under crowding. *Nature Communications, 11*(1), 1687, https://doi.org/10.1038/s41467-020-15386-7.

Huckauf, A., & Heller, D. (2002). What various kinds of errors tell us about lateral masking effects. *Visual Cognition, 9*(7), 889–910, https://doi.org/10.1080/13506280143000548a.

Huckauf, A., & Nazir, T. A. (2007). How odgcrnwi becomes crowding: Stimulus-specific learning reduces crowding. *Journal of Vision, 7*(2):18, 1–12, https://doi.org/10.1167/7.2.18.

Hung, S. C., & Seitz, A. R. (2014). Prolonged training at threshold promotes robust retinotopic specificity in perceptual learning. *The Journal of Neuroscience, 34*(25), 8423–8431, https://doi.org/10.1523/Jneurosci.0745-14.2014.

Hussain, Z., Webb, B. S., Astle, A. T., & McGraw, P. V. (2012). Perceptual learning reduces crowding in amblyopia and in the normal periphery. *The Journal of Neuroscience, 32*(2), 474–480, https://doi.org/10.1523/JNEUROSCI.3845-11.2012.

Intriligator, J., & Cavanagh, P. (2001). The spatial resolution of visual attention. *Cognitive Psychology, 43*(3), 171–216, https://doi.org/10.1006/cogp.2001.0755.

Kalpadakis-Smith, A. V., Goffaux, V., & Greenwood, J. A. (2018). Crowding for faces is determined by visual (not holistic) similarity: Evidence from judgements of eye position. *Scientific Reports, 8*(1), 12556, https://doi.org/10.1038/s41598-018-30900-0.

Kalpadakis-Smith, A. V., Tailor, V. K., Dahlmann-Noor, A. H., & Greenwood, J. A. (2022). Crowding changes appearance systematically in peripheral, amblyopic, and developing vision. *Journal of Vision, 22*(6):3, 1–32, https://doi.org/10.1167/jov.22.6.3.

Keshvari, S., & Rosenholtz, R. (2016). Pooling of continuous features provides a unifying account of crowding. *Journal of Vision, 16*(3):39, 1–15, https://doi.org/10.1167/16.3.39.

Kewan-Khalayly, B., Migó, M., & Yashar, A. (2022). Transient attention equally reduces visual crowding in radial and tangential axes. *Journal of Vision, 22*(9):3, 1–9, https://doi.org/10.1167/jov.22.9.3.

Kewan-Khalayly, B., & Yashar, A. (2022). The role of spatial attention in crowding and feature binding. *Journal of Vision, 22*(13):6, 1–16, https://doi.org/10.1167/jov.22.13.6.

Kewan, B., & Yashar, A. (2021). The role of transient attention in crowding and feature binding. *PsyArXiv*, https://doi.org/10.31234/osf.io/knheg.

Krumhansl, C. L. (1977). Naming and locating simultaneously and sequentially presented letters. *Perception & Psychophysics, 22*(3), 293–302, https://doi.org/10.3758/Bf03199693.

Levi, D. M. (2008). Crowding–an essential bottleneck for object recognition: A mini-review. *Vision Research, 48*(5), 635–654, https://doi.org/10.1016/j.visres.2007.12.009.

Levi, D. M., Hariharan, S., & Klein, S. A. (2002). Suppressive and facilitatory spatial interactions in peripheral vision: Peripheral crowding is neither size invariant nor simple contrast masking. *Journal of Vision, 2*(2), 167–177, https://doi.org/10.1167/2.2.3.

Levi, D. M., & Klein, S. A. (1985). Vernier acuity, crowding and amblyopia. *Vision Research, 25*(7), 979–991, https://doi.org/10.1016/0042-6989(85)90208-1.

Levi, D. M., Klein, S. A., & Hariharan, S. (2002). Suppressive and facilitatory spatial interactions in

foveal vision: Foveal crowding is simple contrast masking. *Journal of Vision, 2*(2), 140–166, https://doi.org/10.1167/2.2.2.

Malania, M., Pawellek, M., Plank, T., & Greenlee, M. W. (2020). Training-induced changes in radial–tangential anisotropy of visual crowding. *Translational Vision Science & Technology, 9*(9), 25, https://doi.org/10.1167/tvst.9.9.25.

Manassi, M., & Whitney, D. (2018). Multi-level crowding and the paradox of object recognition in clutter. *Current Biology, 28*(3), R127–R133, https://doi.org/10.1016/j.cub.2017.12.051.

Maniglia, M., Pavan, A., Cuturi, L. F., Campana, G., Sato, G., & Casco, C. (2011). Reducing crowding by weakening inhibitory lateral interactions in the periphery with perceptual learning. *PLoS One, 6*(10), e25568, https://doi.org/10.1371/journal.pone.0025568.

Motter, B. C., & Simoni, D. A. (2007). The roles of cortical image separation and size in active visual search performance. *Journal of Vision, 7*(2):6, 1–15, https://doi.org/10.1167/7.2.6.

Nandy, A. S., & Tjan, B. S. (2007). The nature of letter crowding as revealed by first- and second-order classification images. *Journal of Vision, 7*(2):5, 1–26, https://doi.org/10.1167/7.2.5.

Nazir, T. A. (1992). Effects of lateral masking and spatial precueing on gap-resolution in central and peripheral vision. *Vision Research, 32*(4), 771–777, https://doi.org/10.1016/0042-6989(92)90192-L.

Parkes, L., Lund, J., Angelucci, A., Solomon, J. A., & Morgan, M. (2001). Compulsory averaging of crowded orientation signals in human vision. *Nature Neuroscience, 4*(7), 739–744, https://doi.org/10.1038/89532.

Pascucci, D., Mastropasqua, T., & Turatto, M. (2015). Monetary reward modulates task-irrelevant perceptual learning for invisible stimuli. *PLoS One, 10*(5), e0124009, https://doi.org/10.1371/journal.pone.0124009.

Pelli, D. G. (1997). The VideoToolbox software for visual psychophysics: Transforming numbers into movies. *Spatial Vision, 10*(4), 437–442, https://doi.org/10.1163/156856897x00366.

Pelli, D. G. (2008). Crowding: A cortical constraint on object recognition. *Current Opinion in Neurobiology, 18*(4), 445–451, https://doi.org/10.1016/j.conb.2008.09.008.

Pelli, D. G., Palomares, M., & Majaj, N. J. (2004). Crowding is unlike ordinary masking: Distinguishing feature integration from detection. *Journal of Vision, 4*(12), 1136–1169, https://doi.org/10.1167/4.12.12.

Petrov, Y., & Meleshkevich, O. (2011a). Asymmetries and idiosyncratic hot spots in crowding. *Vision Research, 51*(10), 1117–1123, https://doi.org/10.1016/j.visres.2011.03.001.

Petrov, Y., & Meleshkevich, O. (2011b). Locus of spatial attention determines inward-outward anisotropy in crowding. *Journal of Vision, 11*(4):1, 1–11, https://doi.org/10.1167/11.4.1.

Petrov, Y., Popple, A. V., & McKee, S. P. (2007). Crowding and surround suppression: Not to be confused. *Journal of Vision, 7*(2):12, 1–9, https://doi.org/10.1167/7.2.12.

Plank, T., Lerner, L., Tuschewski, J., Pawellek, M., Malania, M., & Greenlee, M. W. (2021). Perceptual learning of a crowding task: Effects of anisotropy and optotype. *Journal of Vision, 21*(11):13, 1–11, https://doi.org/10.1167/jov.21.11.13.

Poder, E., & Wagemans, J. (2007). Crowding with conjunctions of simple features. *Journal of Vision, 7*(2):23, 1–12, https://doi.org/10.1167/7.2.23.

Sagi, D. (2011). Perceptual learning in vision research. *Vision Research, 51*(13), 1552–1566, https://doi.org/10.1016/j.visres.2010.10.019.

Scolari, M., Kohnen, A., Barton, B., & Awh, E. (2007). Spatial attention, preview, and popout: Which factors influence critical spacing in crowded displays? *Journal of Vision, 7*(2):7, 1–23, https://doi.org/10.1167/7.2.7.

Shechter, A., & Yashar, A. (2021). Mixture model investigation of the inner–outer asymmetry in visual crowding reveals a heavier weight towards the visual periphery. *Scientific Reports, 11*(1), 2116, https://doi.org/10.1038/s41598-021-81533-9.

Strasburger, H. (2005). Unfocused spatial attention underlies the crowding effect in indirect form vision. *Journal of Vision, 5*(11):8, 1024–1037, https://doi.org/10.1167/5.11.8.

Strasburger, H., Harvey, L. O., & Rentschler, I. (1991). Contrast thresholds for identification of numeric characters in direct and eccentric view. *Perception & Psychophysics, 49*(6), 495–508, https://doi.org/10.3758/Bf03212183.

Strasburger, H., & Malania, M. (2013). Source confusion is a major cause of crowding. *Journal of Vision, 13*(1):24, 1–20, https://doi.org/10.1167/13.1.24.

Strasburger, H., Rentschler, I., & Juttner, M. (2011). Peripheral vision and pattern recognition: A review. *Journal of Vision, 11*(5):13, 1–82, https://doi.org/10.1167/11.5.13.

Sun, G. J., Chung, S. T., & Tjan, B. S. (2010). Ideal observer analysis of crowding and the reduction of crowding through learning. *Journal of Vision, 10*(5):16, 1–14, https://doi.org/10.1167/10.5.16.

Talgar, C. P., Pelli, D. G., & Carrasco, M. (2004). Covert attention enhances letter identification without affecting channel tuning. *Journal of Vision, 4*(1):3, 22–31, https://doi.org/10.1167/4.1.3.

Toet, A., & Levi, D. M. (1992). The two-dimensional shape of spatial interaction zones in the parafovea. *Vision Research, 32*(7), 1349–1357, https://doi.org/10.1016/0042-6989(92)90227-a.

van den Berg, R., Roerdink, J. B., & Cornelissen, F. W. (2010). A neurophysiologically plausible population code model for feature integration explains visual crowding. *PLoS Computational Biology, 6*(1), e1000646, https://doi.org/10.1371/journal.pcbi.1000646.

Wang, R., Cong, L. J., & Yu, C. (2013). The classical TDT perceptual learning is mostly temporal learning. *Journal of Vision, 13*(5):9, 1–9, https://doi.org/10.1167/13.5.9.

Wang, R., Zhang, J. Y., Klein, S. A., Levi, D. M., & Yu, C. (2012). Task relevancy and demand modulate double-training enabled transfer of perceptual learning. *Vision Research, 61*, 33–38, https://doi.org/10.1016/j.visres.2011.07.019.

Wang, R., Zhang, J. Y., Klein, S. A., Levi, D. M., & Yu, C. (2014). Vernier perceptual learning transfers to completely untrained retinal locations after double training: A "piggybacking" effect. *Journal of Vision, 14*(13):12, 1–10, https://doi.org/10.1167/14.13.12.

Whitney, D., & Levi, D. M. (2011). Visual crowding: A fundamental limit on conscious perception and object recognition. *Trends in Cognitive Sciences, 15*(4), 160–168, https://doi.org/10.1016/j.tics.2011.02.005.

Wilkinson, F., Wilson, H. R., & Ellemberg, D. (1997). Lateral interactions in peripherally viewed texture arrays. *Journal of the Optical Society of America A: Optics and Image Science, and Vision, 14*(9), 2057–2068, https://doi.org/10.1364/josaa.14.002057.

Wolford, G. (1975). Perturbation model for letter identification. *Psychological Review, 82*(3), 184–199, https://doi.org/10.1037/0033-295x.82.3.184.

Xiao, L., Zhang, J., Wang, R., Klein, S. A., Levi, D. M., & Yu, C. (2008). Complete transfer of perceptual learning across retinal locations enabled by double

training. *Current Biology, 18*(24), 1922–1926, https://doi.org/10.1016/j.cub.2008.10.030.

Xiong, Y. Z., Yu, C., & Zhang, J. Y. (2015). Perceptual learning eases crowding by reducing recognition errors but not position errors. *Journal of Vision, 15*(11):16, 1–13, https://doi.org/10.1167/15.11.16.

Yashar, A., Chen, J. G., & Carrasco, M. (2015). Rapid and long-lasting reduction of crowding through training. *Journal of Vision, 15*(10):15, 1–15, https://doi.org/10.1167/15.10.15.

Yashar, A., Wu, X., Chen, J., & Carrasco, M. (2019). Crowding and binding: Not all feature dimensions behave in the same way. *Psychological Science, 30*(10), 1533–1546, https://doi.org/10.1177/0956797619870779.

Yeotikar, N. S., Khuu, S. K., Asper, L. J., & Suttle, C. M. (2013). Context and crowding in perceptual learning on a peripheral contrast discrimination task: Context-specificity in contrast learning. *PLoS One, 8*(5), e63278, https://doi.org/10.1371/journal.pone.0063278.

Yeshurun, Y., & Carrasco, M. (1999). Spatial attention improves performance in spatial resolution tasks. *Vision Research, 39*(2), 293–306, https://doi.org/10.1016/s0042-6989(98)00114-x.

Zhang, J.-Y., Zhang, G.-L., Liu, L., & Yu, C. (2012). Whole report uncovers correctly identified but incorrectly placed target information under visual crowding. *Journal of Vision, 12*(7):5, 1–11, https://doi.org/10.1167/12.7.5.

Zhang, J.-Y., Zhang, G.-L., Xiao, L. Q., Klein, S. A., Levi, D. M., & Yu, C. (2010). Rule-based learning explains visual perceptual learning and its specificity and transfer. *The Journal of Neuroscience, 30*(37), 12323–12328, https://doi.org/10.1523/Jneurosci.0704-10.2010.

Zhang, J.-Y., Zhang, G.-L., & Yu, C. (2018). Revealing the mechanisms underlying inner–outer asymmetry and visual crowding. *Journal of Vision, 18*(10), 853, https://doi.org/10.1167/18.10.853.

Zhu, Z., Fan, Z., & Fang, F. (2016). Two-stage perceptual learning to break visual crowding. *Journal of Vision, 16*(6):16, 1–12, https://doi.org/10.1167/16.6.16.